



β -NaFeO₂, a new room-temperature multiferroic material

M. Viret^a, D. Rubi^{a,1}, D. Colson^{a,*}, D. Lebeugle^a, A. Forget^a, P. Bonville^a, G. Dhallene^b, R. Saint-Martin^b, G. André^c, F. Ott^c

^aCEA Saclay, IRAMIS, SPEC (CNRS URA 2464), F-91191 Gif sur Yvette, France

^bUniv. Paris-Sud 11, ICMMO-LPCES (CNRS UMR 8182), F-91405 Orsay, France

^cCEA Saclay, IRAMIS, LLB, F-91191 Gif sur Yvette, France

ARTICLE INFO

Article history:

Received 21 November 2011

Received in revised form 3 May 2012

Accepted 23 May 2012

Available online 30 May 2012

Keywords:

A. Oxides

B. Chemical synthesis

C. X-ray diffraction

D. Ferroelectricity

D. Magnetic properties

ABSTRACT

'Multiferroic' materials possessing simultaneously magnetic and ferroelectric orders are scarce and most of them order at low temperatures. So far, bismuth ferrite, BiFeO₃, is the only reliable room-temperature multiferroic: it is ferroelectric and antiferromagnetic. The absence of a net magnetisation in this compound is a problem when one wants to use the magneto-electric effect to address magnetic information with an electric field for potential applications in spintronic devices. We show here that β -NaFeO₂ is also a multiferroic material at room-temperature but with the most interesting extra property of showing weak ferromagnetism. This makes it a potentially very promising material for applications and a model compound for fundamental studies of the interaction between ferroelectricity and magnetism.

© 2012 Elsevier Ltd. All rights reserved.

1. Introduction

Electricity and magnetism are properties which are closely linked to each other. This link is dynamic in essence, as moving charges generate a magnetic field and a changing magnetic field produces an electric field. This has been known for a long time and forms the basis of Maxwell's equations. In a solid, a similar coupling was first considered by Curie [1] between the equivalent quantities, i.e. magnetisation M and electric polarisation P . This magneto-electric (ME) effect was recently understood to be potentially important for applications, mainly because in spin electronic technology, an efficient control of magnetism by an electric field would allow magnetic information to be written electrically (with low energy consumption) and to be read magnetically.

The ME effect was demonstrated and studied in the 1960s in Russia [2] and since then, many so called 'multiferroic' materials have been identified [3]. However, so far, the magnitude and operating temperatures of any observed ME coupling have been too small for practical applications. In fact, the only known multiferroic material of potential practical interest is bismuth ferrite, BiFeO₃ which is actually antiferromagnetic below $T_N \approx 370$ °C [2] and ferroelectric with a high Curie temperature

($T_c \approx 810$ – 830 °C) [4]. As a result, in recent years, there has been a resurgence in the research conducted on this material [3]. The main problem associated with this compound is the cycloidal arrangement of its moments resulting in zero net magnetisation. This makes the magneto-electric effect (coupling of electrical and magnetic orders) unable to affect a net magnetisation. Instead this interaction is able to toggle the anti-ferromagnetic vector of the G-type arrangement of Fe³⁺ spins [5]. Hence, a way towards using this effect consists in coupling the material with a ferromagnetic layer and take advantage of the interface magnetic exchange coupling [6]. This results in an electric field effect on the magnetisation of the ferromagnetic film. However, it is not entirely clear that this indirect way will lead to a reliable electrical addressing of a magnetisation. Indeed, a direct interaction between electric and (weak) ferromagnetic orders allows an impressive control of the magnetisation by an electric field, but only at low temperature so far [7]. Therefore, there is a crucial need for materials presenting ferroelectricity and a ferromagnetic moment at room-temperature. Here, we demonstrate that β -NaFeO₂ possesses the necessary ingredients, making this compound a promising material.

2. Experimental

2.1. Polycrystalline sample

The pure polycrystalline β -NaFeO₂ compound was prepared by a solid state reaction from a stoichiometric mixture of Na₂CO₃ and

* Corresponding author. Tel.: +33 1 69 08 73 14; fax: +33 1 69 08 87 86.

E-mail address: dorothee.colson@cea.fr (D. Colson).

¹ Now at: GMC, Centro Atómico Constituyentes – CNEA, San Martín, Argentina.

Fe₂O₃. The powder was introduced directly in a tubular furnace at 770 °C for twice 15 h and quenched to room temperature after each calcination. Finally the powder was pelletised and sintered 15 h at 770 °C. Powder X-ray diffraction data were collected at room temperature using a “D8 Advance” diffractometer (Bruker-axs) with Cu K α radiation ($\lambda = 1.5418 \text{ \AA}$) and a scan rate of 0.02° per 20 s. All the samples were found to be single phase. The major problem of this compound is that it is highly hygroscopic and exposure to air gradually decomposes the phase. This is visible with bare eyes because of the appearance of red hematite (Fe₂O₃).

High temperature diffraction measurements reported Section 3.2 were recorded on a ‘D8 Advance’ diffractometer of Bruker-axs using Cu K α radiation and a solid state detector “Sol-X” of Bruker-axs. The XRD system is equipped with a heating chamber with a radiant heater surrounding one sample carrier in alumina and assuring a homogeneous heating by radiation during the measurements, a thermocouple in Pt/Pt–Rh adjusted in direct contact with the sample and Kapton X-ray windows. This device was used under air. Every diagram was recorded for 0.5 h, by steps of 0.02°/s.

2.2. Single crystals

The first single crystals were grown in air from a Na₂CO₃–NaCl flux with the mole ratio Fe₂O₃:Na₂CO₃:NaCl = 1:5:5. Mixture of 5 g of powders were put in an alumina crucible and heated up to 1000 °C, kept for 8 h, and then cooled slowly down to 850 °C at the rate of 5 °C/h. Greenish crystals of typical dimensions 0.4 mm \times 0.1 mm \times 0.05 mm, in the shape of needles were mechanically extracted from the flux. The single-crystal X-ray diffraction data have been collected at 150 K on a Nonius Kappa-CCD area detector diffractometer using graphite-monochromated Mo K α radiation ($\lambda = 0.71073 \text{ \AA}$). A thin platelet (ca. 0.16 mm \times 0.11 mm \times 0.04 mm) has been selected and the structure could be refined to $R = 0.016$ in the orthorhombic space group $Pna2_1$ with the unit cell parameters $a = 5.6793(4) \text{ \AA}$, $b = 7.1243(5) \text{ \AA}$ and $c = 5.3784(2) \text{ \AA}$.

Larger but finely cracked crystals were synthesised in an optical floating-zone furnace (NEC Corporation, Japan) equipped with two lamps installed as infrared radiation sources. The crystal growth was carried out in an enclosed quartz tube where a controlled gas pressure can be applied. For the preparation of NaFeO₂ single crystals, preliminary growth experiments were started on polycrystalline rods. It was observed that crystals become mono-domain after a few centimetres of growth. The feed rod and the growing crystal were rotated at 15 rpm and 20 rpm, respectively, in opposite direction to ensure efficient mixing and uniform temperature distribution in the molten zone. In order to find out the optimised growth parameters, a small excess of Na was needed due to its volatilisation at high temperature and oxygen pressures (1–3 bar) were applied to different growth experiments with different growth rates (1–5 mm/h). In these conditions several crystals of 5 mm in diameter and 50 mm in length have been singled out.

3. Results and discussion

3.1. Magnetic structure

NaFeO₂ can crystallise in different phases [8,9] called α , β and γ . Only the β phase can in principle give rise to ferroelectricity. The neutron powder diffraction experiment was performed at the Orphée reactor (CEA/Saclay, France) at 300 K on the two-axis diffractometer G4.1 ($\lambda = 2.426 \text{ \AA}$; 800-cells-position-sensitive detector), in the 18–98° 2θ range as shown in Fig. 1. The data were analysed using the Rietveld profile method by the Fullprof program

[10], with neutron scattering lengths and Fe³⁺ magnetic form factor taken from that program.

The diagram confirms the orthorhombic crystal symmetry of the compound (space group $Pn2_1a$) [11] and the best refinement (Bragg reliability factors $R_N = 2.0\%$, $R_M = 3.4\%$) evidences an antiferromagnetic G-type structure with Fe³⁺ moments along the b axis of magnitude $3.77(3)\mu_B/\text{Fe}$. This value is smaller than the expected saturated value of $5\mu_B/\text{Fe}$. Mössbauer measurements on the isotope ⁵⁷Fe have also been carried out in order to investigate the state of Fe ions in β -NaFeO₂. The spectrum at 25 °C is composed of six symmetrical absorption lines characteristic of Fe³⁺ in a magnetic environment. The measured hyperfine field of 49T corresponds to a moment of $4.5\text{--}5\mu_B/\text{Fe}$. Therefore, there is a significant discrepancy between the Mössbauer measurements, which are very local in essence, and the neutrons. This could be a signature of a large disorder in a transverse component of magnetisation.

In order to check the macroscopic magnetic behaviour of the compound, we have carried out a series of magnetisation measurements as a function of temperature and magnetic field using a SQUID magnetometer. As shown in Fig. 2, we find that β -NaFeO₂ is weakly ferromagnetic with a spontaneous magnetisation of $5 \times 10^{-4} \mu_B/\text{cell}$ at room-temperature (a value far below the

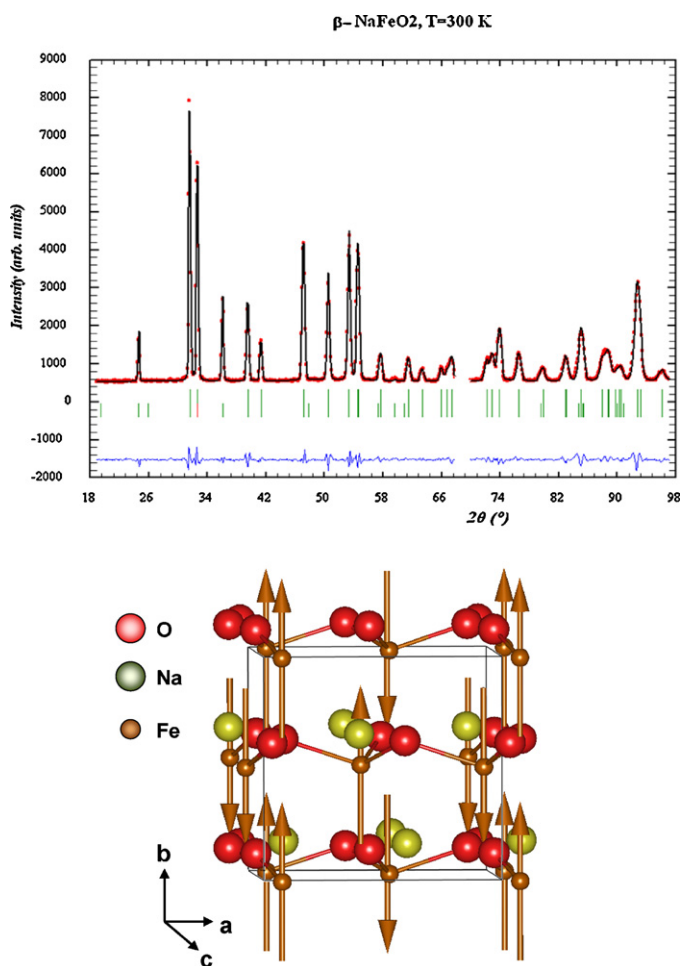


Fig. 1. (a) Refinement of the neutron powder diagram of NaFeO₂ recorded at 300 K with the G4.1 diffractometer ($\lambda = 2.426 \text{ \AA}$) in Saclay. Experimental data are represented by open circles, the calculated profile by a continuous line, and the allowed structural (upper row) and magnetic (lower row) Bragg reflections by vertical marks. The difference between the experimental and calculated profiles is displayed in blue at the bottom of the graph. (b) Schematics of the obtained magnetic unit cell.

resolution of the neutron powder diffraction technique). The high-field slope is due to a progressive canting of the antiferromagnetic sublattices and its susceptibility is found to be around 10^{-3} emu/mole, of the same order of magnitude as what can be theoretically expected from the Néel temperature ($T_N = 723$ K [2]).

The value for the spontaneous magnetisation could be explained by a canting of the antiferromagnetic sublattices by an angle of 0.003° or a not complete disorder of the transverse magnetisation. We would like to point out here that this small component is unlikely to come from a parasitic phase because it is reproducibly measured in several high purity powders prepared in slightly different conditions. Moreover, the temperature dependence of magnetisation shown in Fig. 2(b) does not provide any evidence for the existence of ferromagnetic parasitic phases below 300 K. Thus, only Fe_3O_4 could possibly generate such a room-temperature hysteresis, but it is very unlikely to be formed as the synthesis is not performed under a reducing atmosphere, which would allow the formation of ferromagnetic phases with mixed valences $\text{Fe}^{2+}/\text{Fe}^{3+}$. Extensive electron microprobe analyses on many samples did not reveal the existence of parasitic phases, except sometimes the antiferromagnetic $\text{Na}_3\text{Fe}_5\text{O}_9$ phase. These magnetic properties could therefore be a consequence of superexchange and Dzyaloshinskii–Moria [12] interactions. The latter can also depend on the coupling between local spins and electrical polarisation [13,14]. We note however, that the magneto-electric

interaction has a clear tendency to generate periodic structures [15] like the cycloid in BiFeO_3 . A detailed study of the canting direction in the unit cell would be very welcome but this must await the synthesis of reasonably sized single crystals. What can be said so far is that the basic interaction is superexchange but because the Fe–O–Fe angle is only 126° , quite far from the optimal 180° for the antiferromagnetic superexchange coupling, the non perfect orbital overlap allows for a slight canting to appear.

3.2. Ferroelectric properties

The ferroelectric character of $\beta\text{-NaFeO}_2$ is much harder to evidence because of materials problems. In a first step we had to measure ceramics which were not dense enough (to prevent them from being brittle), which implies a limitation on the minimum thickness we could make and therefore on the maximum electrical field we could apply. Moreover, $\beta\text{-NaFeO}_2$ is hygroscopic as well as sensitive to CO_2 , and after several minutes in air, the pellets change colour while an irreversible phase transition occurs. It is most likely that humidity penetrates through grain boundaries and leakage currents are seen to evolve with time, increasing steadily.

The measurements were carried out in the simplest possible way, i.e. we swept a voltage and measured a current with a picoammeter. This measures the derivative of the $P(E)$ hysteresis cycle along with the leakage currents. A full cycle is obtained typically in 5 min (i.e. a very low sweep rate that minimises the capacitive effects). When measuring $\beta\text{-NaFeO}_2$, switching is not systematically observed during the first few minutes and a clear ferroelectric behaviour is only obtained after four or five cycles. We think that this is due to grain boundaries turning more conducting as water or CO_2 is getting in from the surface. This gradually reduces the effective thickness of the ferroelectric and after a little while, the electric field generated by our maximum applied voltage (500 V) reaches the coercive field of the material and switching occurs. Because humidity is detrimental to leakage currents, the samples also become more conducting until it is not possible to apply high voltages anymore. Therefore, the measurements are usually optimal after typically 15 min in air and in a time window of about one hour. We have verified the hypothesis of conducting grain boundaries by re-drying the sintered pellets after one hour (using silica gel) and re-starting the whole process. This procedure is found to work for a reasonable proportion of the samples, but the phase changes are not completely reversible. For the electrical measurements, in the simplest case, our samples are pinched between two flat 2 mm^2 electrodes using a spring system. We also tried using Pt or Au electrodes deposited on each side of the pellet, but electrical switching was never obtained. In that case, humidity cannot get in and the coercive fields could never be reached in the measurements. Despite all this, about 70% of our pellets show an electric switching behaviour (i.e. about 40 samples). A representative $I(V)$ cycle (obtained in the first switching events) is shown in Fig. 3(a), while Fig. 3(b) shows the estimated polarisation (obtained after integration of the $I-V$ curve) as a function of the electrical field. In order to check that the hysteresis observed in the $I-V$ curves is indeed related to ferroelectric switching we have performed two additional experiments. In the first one, shown in Fig. 3(c), we have cycled the electrical field from 0 to $E_{\text{max}} = +6$ kV/cm and then to zero again, for two consecutive runs. The fact that the first cycle shows hysteresis while the second one does not, provides evidence for a ferroelectric behaviour. It is indeed expected that ferroelectric switching takes place during the first cycle after a large negative electric field was applied while in the second one, ferroelectric domains are already switched and hysteresis does not show up. In a second experiment we have recorded the current as a function of time at fixed electrical fields, going from zero to 2 kV/cm, then to -2 kV/cm and then to zero

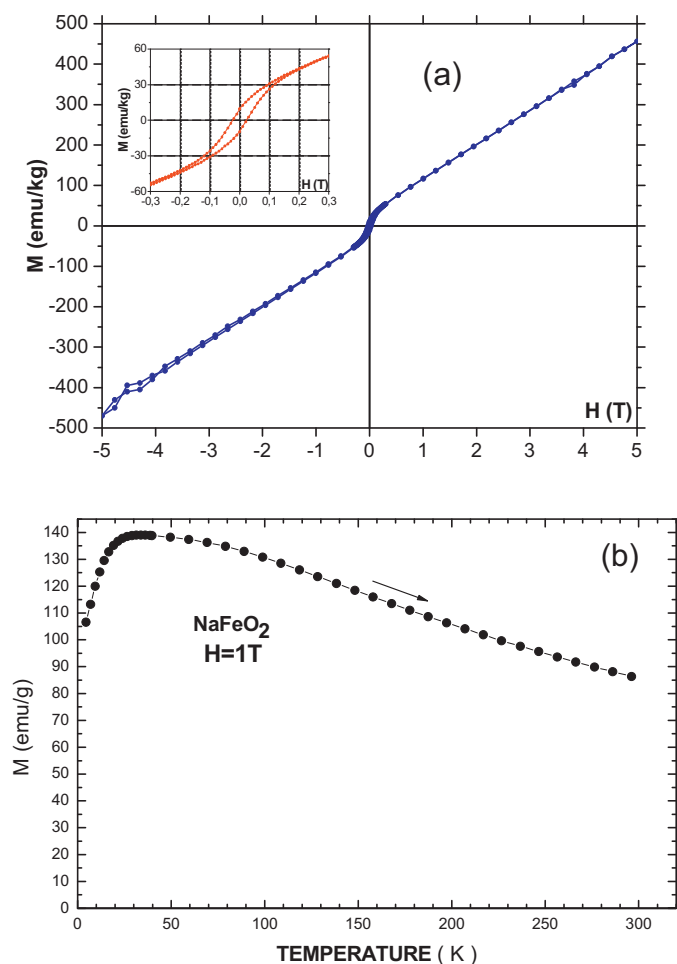


Fig. 2. (a) Hysteresis cycle at room-temperature for $\beta\text{-NaFeO}_2$. A weak ferromagnetic contribution is present, superimposed to a linear antiferromagnetic susceptibility. The magnetic moment corresponds to $5 \times 10^{-4} \mu_B/\text{cell}$, i.e. a small canting angle of 0.003° . (b) Temperature dependence of the magnetisation at 1 T where no signature of ferromagnetic parasitic phases can be seen.

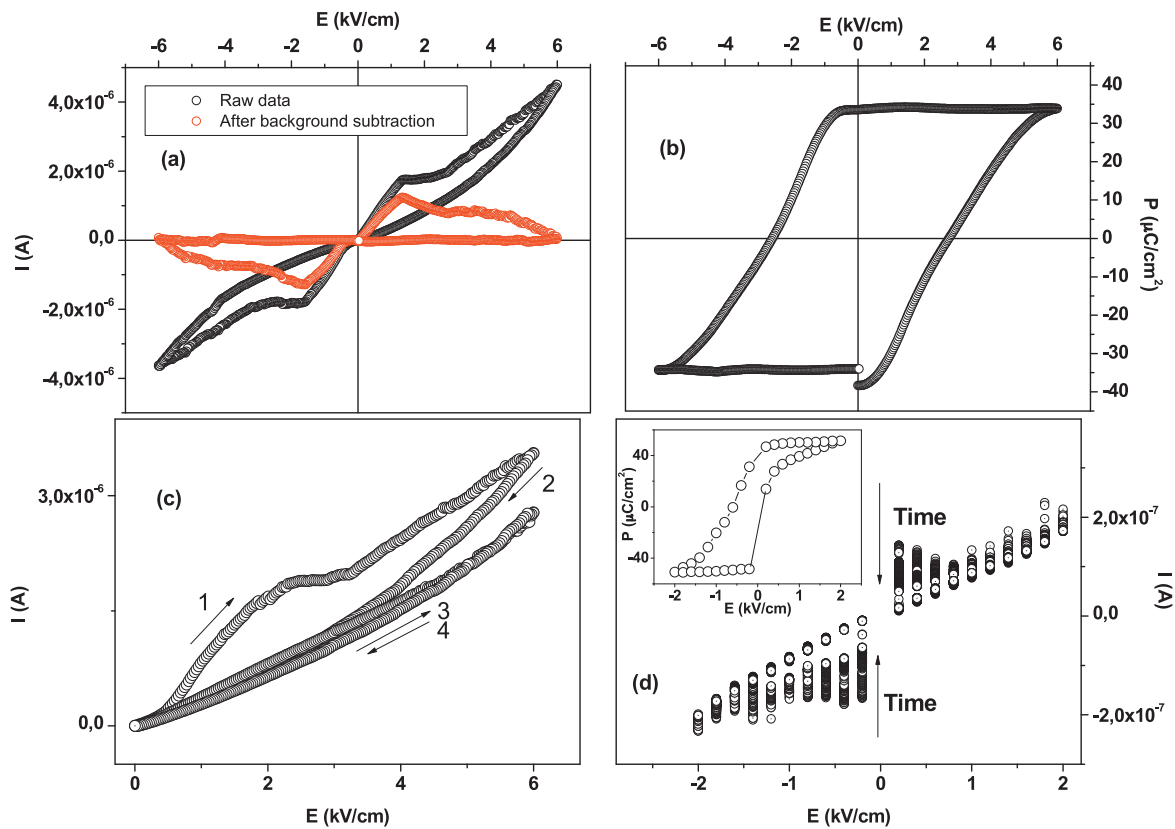


Fig. 3. (a) Typical hysteresis cycle recorded after a progressive evolution of the reversal during field cycling for about 20 min (accompanied by a slow increase of the leakage current). (b) Hysteresis cycle extracted by integration of the $I(V)$ curve of (a) where the leakage currents have been subtracted by taking the difference with the measured signals as the voltage is swept back from saturation. The electrical polarisation is estimated around $40 \mu\text{C}/\text{cm}^2$. (c) Difference between the hysteresis obtained during electrical switching and the reversible behaviour when the sample has not been previously poled negatively. (d) Time measurements of the discharging at each step during electric field reversal. The integrated signals give the switching polarisation showing the difference between the electric reversal and the return from saturation.

again, with a step of $0.2 \text{ kV}/\text{cm}$. As shown in Fig. 3(d), it is found that the intensity of the current decreases with time, indicating a progressive discharging of switching currents. After integrating the corresponding $I(t)$ at different voltages, we have obtained the evolution of the polarisation with electrical fields observed in the inset of Fig. 3(d). Although it can safely be asserted that $\beta\text{-NaFeO}_2$ is indeed ferroelectric, it is hard to quantitatively evaluate its polarisation. In these measurements, the amount of charges passing through the circuit due to polarisation reversal is obtained by integrating the current peaks at the switching field. This is proportional to the value of polarisation provided the discharging area is known. In our case, this is not as obvious as it normally is because our contact is basically done by a grain boundary network. In that case, the effective area can be much more than the mere surface of the pellet. Moreover, it varies with time as humidity gets in. Postulating that the first obtained hysteresis cycles are the most reliable ones (before the contact network becomes 'very fractal') we have found an average polarisation of around $40 \mu\text{C}/\text{cm}^2$, reaching in some samples values as high as $90 \mu\text{C}/\text{cm}^2$. The latter value is consistent with what one gets when postulating the pure ionic charges for the ions: Fe^{3+} , Na^+ and O^{2-} and the coordinates extracted from the X-ray and neutron measurements.

In order to better measure the intrinsic properties of the compound, single crystals were grown by a flux growth method as well as a floating zone technique. With the first technique, the obtained crystals were too small to be measured electrically. The floating zone technique allows to obtain millimetre sized crystals, but unfortunately these were densely cracked and presented large leakage currents. Thus, no reasonable voltages could be applied and $P(E)$ loops could

not be recorded. However, after a meticulous polishing, a crystal was observed in polarised light with a microscope in reflectivity mode where different domains could be seen (Fig. 4). The contrast between domains provides evidence for birefringent properties, an observation consistent with the presence of domains of different spontaneous polarisations.

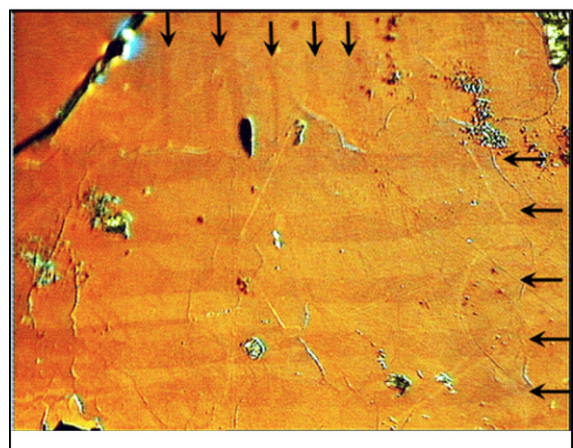


Fig. 4. Photograph of a NaFeO_2 crystal obtained by the floating zone method (rate of $3 \text{ mm}/\text{h}$, $P_{\text{O}_2} = 3 \text{ bar}$) examined after a meticulous polishing under a polarising microscope with polychromatic light. The crystal is finely cracked but several horizontal and vertical stripes can be seen (indicated by black arrows). The contrast between bright and dark regions is likely to originate from the birefringence of different polarisation domains.

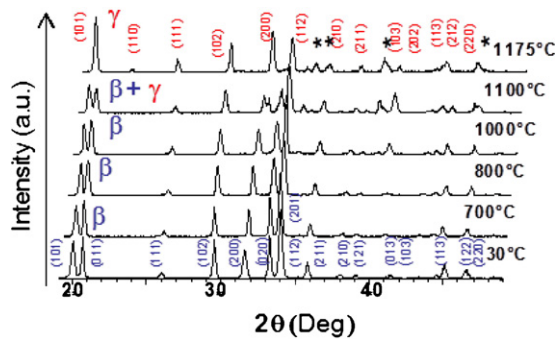


Fig. 5. XRD patterns (Cu $K\alpha$) of the NaFeO_2 powder sample as a function of temperature showing the transformation near 1100°C from the orthorhombic β phase to the tetragonal γ phase associated to a likely loss of ferroelectricity. The patterns have been indexed using Ref. [11]. At 1175°C the main diffraction peaks are identified as the γ phase structure, only some diffraction peaks (*) are assigned to the alumina holder and the platinum thermocouple.

In order to estimate the ferroelectric ordering temperature, we have followed by powder X-ray diffraction the temperature evolution of the NaFeO_2 structure (Fig. 5). The lattice symmetry of the ferroelectric β phase changes from orthorhombic ($Pna2_1$) to the tetragonal ($P4_12_12$) γ phase with higher symmetry which should not be ferroelectric anymore. Hence, this transformation should be accompanied with the loss of spontaneous polarisation and the γ phase should be paraelectric. This phase transformation is found around 1100°C which we then associate to the ferroelectric Curie temperature. Therefore, $\beta\text{-NaFeO}_2$ has a high ferroelectric ordering temperature which does not coincide with its magnetic Néel temperature of 450°C .

4. Conclusion

In conclusion, we show here that $\beta\text{-NaFeO}_2$ is a ferroelectric and weak ferromagnetic compound with ordering temperatures largely above room-temperature. Although its big drawback is

to be overly sensitive to humidity and CO_2 , this compound has the potential to become a first class candidate for applications in spintronics, for example in ferroelectric/magnetic memory elements where electrical writing and magnetic reading would be the best combination regarding energy consumption and reliability for random access memory storage. However, many things have yet to be investigated, and in particular the essential presence of the magneto-electric effect in $\beta\text{-NaFeO}_2$. This will have to await the synthesis of good quality and large enough single crystals.

Acknowledgements

DC would like to thank P. Thuéry for his help in X-ray diffraction measurements on single crystals. MV, DC, and PB would like to acknowledge support from the French Agence Nationale pour la Recherche, contract MELOIC (ANR-08-P196-36).

References

- [1] P. Curie, J. Phys. 3 (1894) 393.
- [2] See G.A. Smolenskii, I.E. Chupis, Sov. Phys. Uspekhi, 25 (1982) 475; Y.N. Venevtsev, V.V. Gagulin, Ferroelectrics 162 (1994) 23, and references therein.
- [3] M. Fiebig, J. Phys. D 38 (2005) 123; W. Eerenstein, N.D. Mathur, J.F. Scott, Nature 442 (2006) 759.
- [4] R.T. Smith, G.D. Achenbach, R. Gerson, W.J. James, J. Appl. Phys. 39 (1) (1968) 70.
- [5] D. Lebeugle, D. Colson, A. Forget, M. Viret, A. Bataille, A. Goukassov, Phys. Rev. Lett. 100 (2008) 227602.
- [6] H. Béa, M. Bibes, F. Ott, B. Dupé, X.-H. Zhu, S. Petit, S. Fusil, C. Deranlot, K. Bouzehouane, A. Barthélémy, Phys. Rev. Lett. 100 (2008) 017204.
- [7] Y. Tokunaga, N. Furukawa, H. Sakai, Y. Taguchi, T. Arima, Y. Tokura, Nat. Mater. 8 (2009) 558.
- [8] F. Bertaut, P. Blum, Comptes rendus de l'Académie des Sciences Séance du 2 août 1954.
- [9] J. Théry, R. Collongues, Comptes rendus de l'Académie des Sciences Séance du 1er décembre 1958.
- [10] J. Rodriguez-Carvajal, Physica B 192 (1993) 55.
- [11] I.E. Grey, R.J. Hill, A.W. Hewat, Z. Kristallogr. 193 (1990) 51.
- [12] I.E. Dzyaloshinskii, Sov. Phys. JETP 10 (1959) 628; T. Moriya, Phys. Rev. 120 (1960) 91.
- [13] H. Katsura, N. Nagaosa, A.V. Balatsky, Phys. Rev. Lett. 95 (2005) 057205.
- [14] I.A. Sergienko, E. Dagotto, Phys. Rev. B 73 (2006) 094434.
- [15] M. Mostovoy, Phys. Rev. Lett. 96 (2006) 067601.